

Simultaneous description of low-lying positive and negative parity bands in heavy even-even nuclei

H. G. Ganev¹

¹*Joint Institute for Nuclear Research, 141980 Dubna, Russia*

The low-lying spectra including the first few excited positive and negative parity bands of some heavy even-even nuclei from the rare earth and actinide mass regions are investigated within the framework of the symplectic Interacting Vector Boson Model with $\text{Sp}(12, R)$ dynamical symmetry group. Symplectic dynamical symmetries allow the change of the number of excitation quanta or phonons building the collective states providing for larger representation spaces and richer subalgebraic structures to incorporate more complex nuclear spectra. The theoretical predictions for the energy levels and the electromagnetic transitions between the collective states of the ground state band and $K^\pi = 0^-$ band are compared with experiment and some other collective models incorporating octupole and/or dipole degrees of freedom. The energy staggering which is a sensitive indicator of the octupole correlations in the even-even nuclei is also calculated and compared with experiment. The results obtained for the energy levels, energy staggering and transition strengths reveal the relevance of the used dynamical symmetry of the model for the simultaneous description of both positive and negative parity low-lying collective bands.

PACS number(s): 21.10.Re, 21.60.Fw, 23.20.Lv, 27.60.+j

I. INTRODUCTION

It is well known [1],[2] that in some mass regions several bands of negative parity are observed in the low-lying nuclear spectra in even-even nuclei, like $K^\pi = 0^-$, 1^- and 2^- bands. The most well-studied of them is the $K^\pi = 0^-$ band, usually interpreted as an octupole vibrational band, connected to the ground state band (GSB) by enhanced $E1$ transitions.

Negative parity states have been described within different approaches mainly by inclusion of octupole or/and dipole degrees of freedom. The bands of negative parity states are often associated with the reflection asymmetry in the intrinsic frame of reference. In the geometrical approach this is achieved by including of the $\alpha_{30} \equiv \beta_3$ deformation [3]. In the Interacting Boson Model (IBM) [4] the description of negative states requires the introduction of f or/and p bosons with negative parity in addition to the standard s and d bosons ($spdf$ -IBM) [5],[6]. An alternative interpretation of the low-lying negative parity states has been provided in different cluster models [7]-[8] in which the dipole degrees of freedom are related with the relative motion of the clusters. Based on the Bohr Hamiltonian different critical point symmetries (CPS) including axial quadrupole and octupole deformations have been proposed [9]-[11], [12] extending the concept of CPS introduced for the description of positive parity states.

In this paper we present an algebraic approach, complementary to the $spdf$ -IBM [5], for the unified description of the low-lying positive and negative parity bands in some even-even nuclei from the rare earth and actinide mass regions within the framework of the symplectic Interacting Vector Boson Model (IVBM) with $\text{Sp}(12, R)$ dynamical symmetry group [13]. The present work is an

extension of the approach proposed in Ref.[14] for the description of the ground state band and the "octupole" ($K^\pi = 0^-$) band, often treated as a single ground state alternating parity band. In this way we investigate simultaneously the first few low-lying negative parity bands ($K^\pi = 0^-$, 1^- and 2^-) together with the first few positive parity (ground state, β and γ) bands. It is shown that the negative parity bands arise along with the positive bands without the introduction of any additional collective degrees of freedom. Additionally, we calculate the strengths of the intraband $E2$ transitions in both the GSB and $K^\pi = 0^-$ band, as well as the interband $E1$ transitions connecting the states of these two bands. The energy staggering of the ground state alternating band which is a sensitive indicator of the octupole correlations in the even-even nuclei is also calculated and compared with experiment.

II. THEORETICAL FRAMEWORK

A. The IVBM

It was suggested by Bargmann and Moshinsky [15],[16] that two types of bosons are needed for the description of nuclear dynamics. It was shown there that the consideration of only two-body system consisting of two different interacting vector particles will suffice to give a complete description of N three-dimensional oscillators with a quadrupole-quadrupole interaction. The latter can be considered as the underlying basis in the algebraic construction of the *phenomenological* IVBM [13].

The algebraic structure of the IVBM is realized in terms of creation and annihilation operators of two kinds of vector bosons $u_m^\dagger(\alpha)$, $u_m(\alpha)$ ($m = 0, \pm 1$), which differ in an additional quantum number $\alpha = \pm 1/2$ (or $\alpha = p$ and n)—the projection of the T -spin (an analogue to the F -spin of IBM-2 or the I -spin of the particle-hole

IBM). All bilinear combinations of the creation and annihilation operators of the two vector bosons generate the boson representations of the non-compact symplectic group $Sp(12, R)$:

$$F_M^L(\alpha, \beta) = \sum_{k,m} C_{1k1m}^{LM} u_k^+(\alpha) u_m^+(\beta), \quad (1)$$

$$G_M^L(\alpha, \beta) = \sum_{k,m} C_{1k1m}^{LM} u_k(\alpha) u_m(\beta), \quad (2)$$

$$A_M^L(\alpha, \beta) = \sum_{k,m} C_{1k1m}^{LM} u_k^+(\alpha) u_m(\beta), \quad (3)$$

where C_{1k1m}^{LM} , which are the usual Clebsch-Gordan coefficients for $L = 0, 1, 2$ and $M = -L, -L+1, \dots, L$, define the transformation properties of (1),(2) and (3) under rotations. The number preserving operators (3) generate the $U(6)$ group, while by adding the pair creation (1) and annihilation (2) operators we generate the non-compact $Sp(12, R)$ which is the dynamical group of the IVBM. Its irreducible representations are infinite dimensional. We also introduce the following notations for the two bosons: $u_m^\dagger(\alpha = 1/2) = p_m^\dagger$ and $u_m^\dagger(\alpha = -1/2) = n_m^\dagger$.

Symplectic dynamical symmetries allow the change of the number of bosons, elementary excitations or phonons N , providing for richer subalgebraic structures and larger representation spaces to accommodate more structural effects. Dynamical symmetry group $Sp(12, R)$ contains both compact and non-compact substructures, defined by different reduction chains.

B. Dynamical symmetry

We consider the following chain [13],[14]

$$Sp(12, R) \supset U(6) \supset SU(3) \otimes U(2) \supset SO(3) \otimes U(1), \\ [N]_6 \quad (\lambda, \mu) \longleftrightarrow (N, T) \quad K \quad L \quad T_0 \quad (4)$$

where below the different subgroups the quantum numbers characterizing their irreducible representations are given. The generators of different subgroups in Eq.(4) are expressed in terms of the number-preserving operators (3). The number operator

$$N = p^\dagger \cdot p + n^\dagger \cdot n = N_p + N_n \quad (5)$$

is the linear invariant of the $U(6)$, as well as $U(3)$ and $U(2)$ algebras. The $SU(3)$ algebra is generated by the components of the angular momentum

$$L_M = -\sqrt{2} \sum_{\alpha} A_M^1(\alpha, \alpha) \quad (6)$$

and Elliott's quadrupole

$$Q_M = \sqrt{6} \sum_{\alpha} A_M^2(\alpha, \alpha) \quad (7)$$

operators. The T -spin operators:

$$T_{+1} = -\frac{1}{\sqrt{2}} p^\dagger \cdot n, \quad (8)$$

$$T_{-1} = \frac{1}{\sqrt{2}} n^\dagger \cdot p, \quad (9)$$

$$T_0 = \frac{1}{2} (p^\dagger \cdot p - n^\dagger \cdot n) \quad (10)$$

together with the number operator (5) generate the $U(2)$ algebra.

Within the symmetric irreducible representation $[N]_6$ of $U(6)$ the groups $SU(3)$ and $U(2)$ are mutually complementary [17], i.e. the quantum numbers (λ, μ) are related with (N, T) in the following way $N = \lambda + 2\mu$ and $T = \lambda/2$. Making use of the latter we can write the basis as

$$|[N]_6; (\lambda, \mu); K, L; T_0\rangle = |(N, T); K, L; T_0\rangle \quad (11)$$

The ground state of the system is:

$$|0\rangle = |(N=0, T=0); K=0, L=0; T_0=0\rangle \quad (12)$$

which is the vacuum state for the $Sp(12, R)$ group.

The basis states associated with the even irreducible representation of the $Sp(12, R)$ can be constructed by the application of powers of raising generators $F_M^L(\alpha, \beta)$ of the same group on the vacuum. Each raising operator will increase the number of bosons N by two. The resulting infinite set of basis states so obtained is denoted as (11) and is shown in Table I. Each row (fixed N) of the table corresponds to a given $U(6)$ irrep, whereas each cell represents the $SU(3)$ irrep contained in the corresponding $U(6)$ one. For fixed N , the possible values for the T -spin are $T = \frac{N}{2}, \frac{N}{2} - 1, \dots, 0$ and are given in the column next to the respective value of N . Thus when N and T are fixed, $2T + 1$ equivalent representations (λ, μ) of the group $SU(3)$ arise. Each of them is labeled by the eigenvalues of the operator $T_0 : -T, -T + 1, \dots, T$, defining the columns of Table I. The values of the angular momentum contained in a certain $SU(3)$ representation (λ, μ) are obtained by means of standard reduction rules for the chain $SU(3) \supset SO(3)$ [18]:

$$K = \min(\lambda, \mu), \min(\lambda, \mu) - 2, \dots, 0 \quad (1) \\ L = \max(\lambda, \mu), \max(\lambda, \mu) - 2, \dots, 0 \quad (1); K = 0 \quad (13) \\ L = K, K + 1, \dots, K + \max(\lambda, \mu); K \neq 0.$$

The multiplicity index K appearing in this reduction is related to the projection of L in the body fixed frame and is used with the parity (π) to label the different bands (K^π) in the energy spectra of the nuclei.

C. The Hamiltonian

We use the following Hamiltonian [14]:

$$H = aN + bN^2 + \alpha_3 T^2 + \beta_3 L^2 + \alpha_1 T_0^2 \quad (14)$$

TABLE I: Classification of the basis states.

N	T	$T_0 \dots$	-3	-2	-1	0	1	2	3	\dots
0	0					(0, 0)				
2	1				(2, 0)	(2, 0)	(2, 0)			
	0					(0, 1)				
4	2			(4, 0)	(4, 0)	(4, 0)	(4, 0)	(4, 0)		
	1				(2, 1)	(2, 1)	(2, 1)			
	0					(0, 2)				
6	3		(6, 0)	(6, 0)	(6, 0)	(6, 0)	(6, 0)	(6, 0)	(6, 0)	
	2			(4, 1)	(4, 1)	(4, 1)	(4, 1)	(4, 1)		
	1				(2, 2)	(2, 2)	(2, 2)			
	0					(0, 3)				
\dots	\dots	\dots	\dots	\dots	\dots	\dots	\dots	\dots	\dots	\dots

expressed in terms of the first and second order invariant operators of the different subgroups in the chain (4). It is obviously diagonal in the basis (11) and its eigenvalues are just the energies of the nuclear system:

$$E(N, L, T, T_0) = aN + bN^2 + \alpha_3 T(T+1) + \beta_3 L(L+1) + \alpha_1 T_0^2. \quad (15)$$

The energy of the ground state (12) of the system is obviously 0.

III. APPLICATION

In our application, the most important point is the identification of the experimentally observed states with a certain subset of the basis states (11). In this regard, the following two points are of importance. First, as we noted the irreducible representations of $\text{Sp}(12, R)$ are infinite dimensional. Then the truncation of the model space to a finite-dimensional subspace of physically meaningful basis states revealing the collective properties of states described is required. It turns out that such an appropriate set of states is given by the so called "stretched states" [19], which represent dominant $\text{SU}(3)$ multiplets in the low-lying collective states [19]. In the present ap-

plication we use the following type of stretched states defined as the $\text{SU}(3)$ states of the type $(\lambda, \mu) = (\lambda_0, \mu_0 + k)$, where $k = 0, 2, 4, \dots$. In the symplectic IVBM the change of the number k , which is related in the applications to the angular momentum L of the states, gives rise to the collective bands.

The second point concerns the parity of the state. We assume that the one type of two vector bosons, say p -boson, transforms under space reflections as a pseudovector, while the other n -boson - transforms as a vector. The latter assumes that the creation operators of the two vector bosons p_m^\dagger and n_m^\dagger can be considered as acting separately in the two adjacent major oscillator shells of opposite parity, creating in this way two different elementary excitations ("Elliott quarks", see [20]) with opposite parity from which the collective states are built out. So, we define the parity of the considered collective state as $\pi = (-1)^{N_n}$ which generalizes our previous definition of the parity $\pi = (-1)^T$ given in Ref.[14]. This allows us to describe both positive and negative parity states in the IVBM on the same footing without introducing of any additional collective degrees of freedom.

In this way for example, the states of the ground state band are mapped onto the $\text{SU}(3)$ multiplets $(0, L)$ ($T = 0, T_0 = 0$) with $L = 0, 2, 4, \dots$, whereas those of $K^\pi = 0^-$ band onto the $\text{SU}(3)$ multiplets $(2, L)$ ($T = 1, T_0 = 1$) with $L = 1, 3, 5, \dots$. The latter mapping slightly differs from that used in Ref.[14] with $(T = 1, T_0 = 0)$ because of the parity definition. We note that although the set of used $\text{SU}(3)$ states in [14] and in the present approach is identical, in order to take proper into account the parity of the collective states, we need appropriate values of both T and T_0 . Note that the $\text{SU}(3)$ degeneracy within a given $\text{U}(6)$ irrep is lifted by its mutually complementary group $\text{U}(2)$. The same type of the stretched states $(\lambda, \mu) = (\lambda_0, \mu_0 + k)$ are also used for other bands under consideration.

A. The energy spectra

We consider the first few excited low-lying positive (ground state, β, γ) and negative ($K^\pi = 0^-, 1^-, 2^-$) parity bands of some nuclei from the rare earth and light actinide regions for which there is enough experimental data on $E1$ and $E2$ transitions.

In Fig.1 we compare our theoretical predictions for the energies of the first excited positive and negative parity bands observed in ^{152}Sm , ^{154}Sm , ^{148}Nd , ^{150}Nd , ^{226}Ra and ^{230}Th with experiment [1] and the results obtained by the diagonalization of the $spdf$ -IBM Hamiltonian [21] (^{152}Sm , ^{154}Sm), [22] (^{150}Nd), [23] (^{226}Ra , ^{230}Th). For the

^{152}Sm , ^{150}Nd and ^{226}Ra isotopes, the predictions of the CPS approach [11],[10] in which the octupole degrees of freedom are included together with the quadrupole ones are also shown. In the case of ^{226}Ra the results of the pure $\text{SU}(3)$ dynamical limit of the $spdf$ -IBM are shown as well. The calculations in the $\text{SU}(3)$ limit of $spdf$ -IBM are performed using the Hamiltonian and matrix elements given in [24]. The values of the model parameters obtained in the fitting procedure are given in Table II.

The ^{152}Sm and ^{150}Nd isotopes in the positive parity part (GSB and β band) of the spectrum are considered

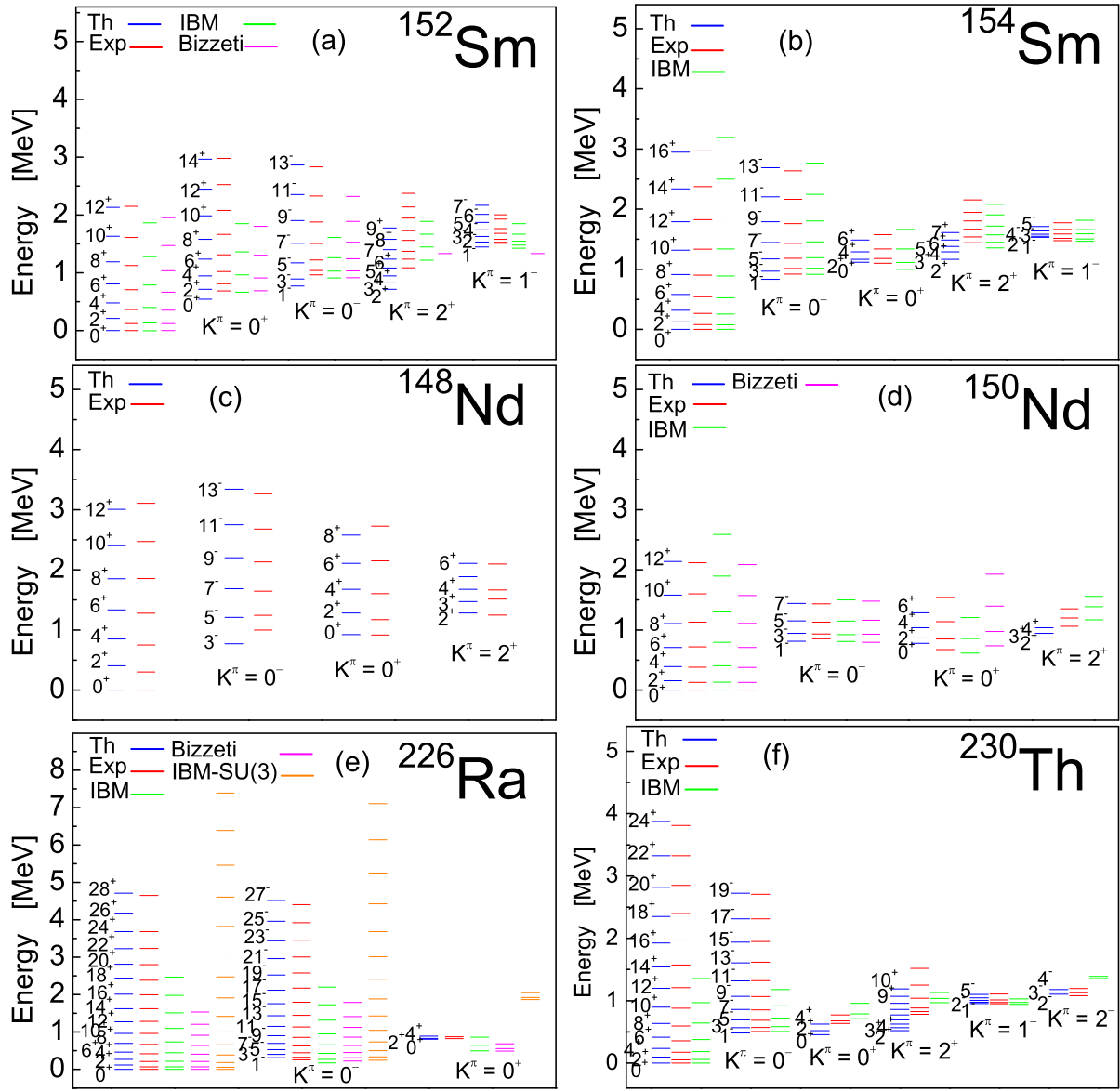


FIG. 1: (Color online) Comparison of the theoretical energies for the low-lying positive and negative parity bands in ^{152}Sm , ^{154}Sm , ^{148}Nd , ^{150}Nd , ^{226}Ra and ^{230}Th with experiment and some other collective models incorporating octupole or/and dipole degrees of freedom.

TABLE II: The values of the model parameters (in MeV).

Nucleus	a	b	α_3	β_3	α_1
^{152}Sm	0.02792	-0.00176	0.10948	0.01551	0.46287
^{154}Sm	0.01476	-0.00153	0.06864	0.01486	0.63245
^{148}Nd	0.09149	-0.00155	0.09725	0.01094	-0.18550
^{150}Nd	0.01572	-0.00413	0.95750	0.02656	-1.1522
^{226}Ra	0.01581	-0.00278	0.12640	0.01600	0.00523
^{230}Th	0.01248	-0.00204	0.15437	0.01331	0.13035

as examples of the X(5) critical point symmetry [25]. The

nucleus ^{226}Ra is considered in the literature as possessing stable octupole shape. The ^{230}Th is considered as an octupole soft nucleus in a recent constrained self-consistent relativistic mean-field calculations [26].

One sees that the IVBM describes reasonably well the structure of low-lying excited states of the first few bands of positive and negative parity up to high angular momenta for the all nuclei under consideration. Note that in the case of ^{226}Ra , the experimental data show large deviations from the rotational $L(L+1)$ rule (SU(3) limit of the spdf-IBM) for both the ground state and $K^\pi = 0^-$ bands despite the fact that $R_{4/2} = 3.13$.

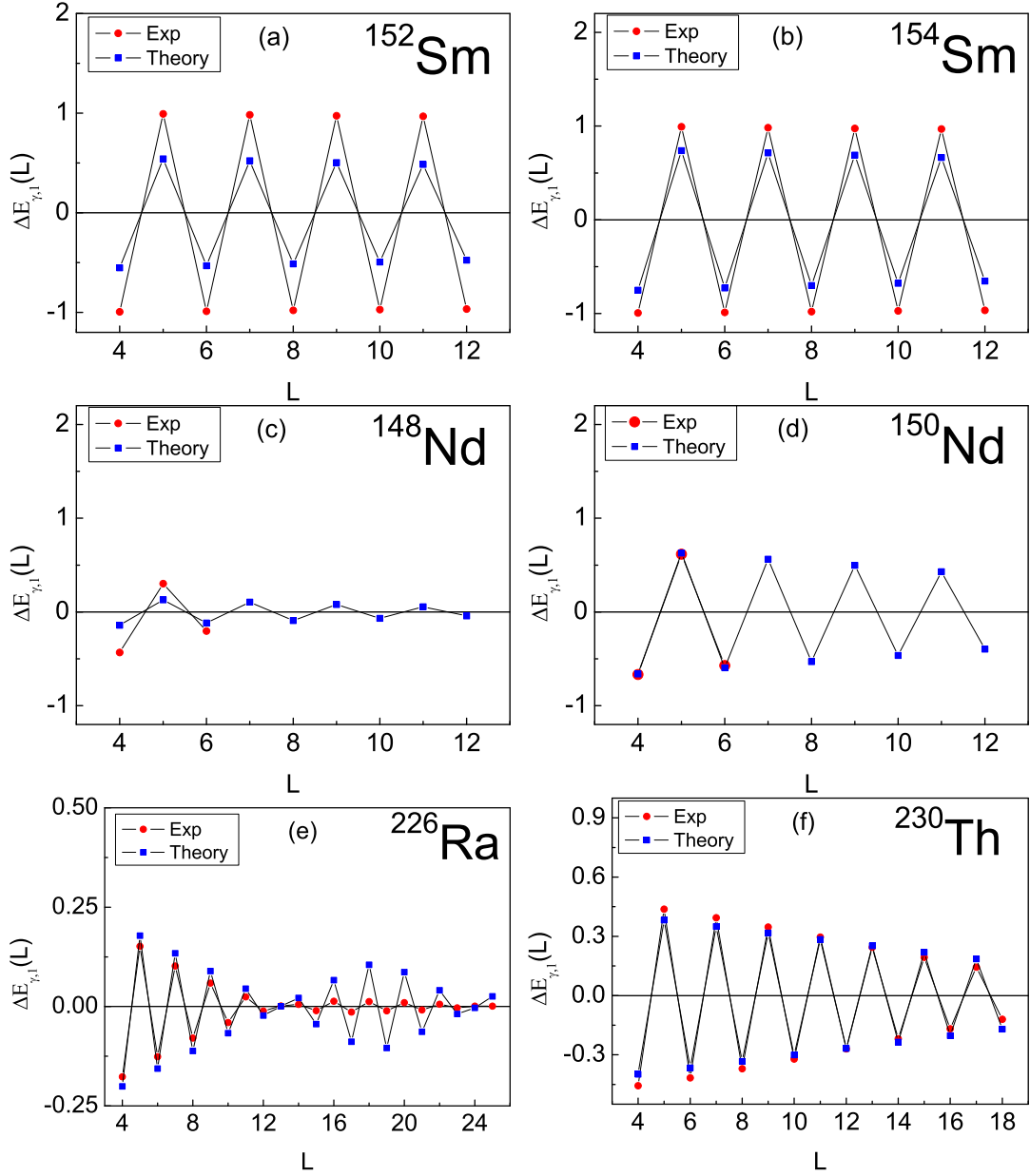


FIG. 2: (Color online) Theoretical and experimental staggering function $\Delta E_{\gamma,1}(L)$ (19) in ^{152}Sm , ^{154}Sm , ^{148}Nd , ^{150}Nd , ^{226}Ra and ^{230}Th .

B. The energy staggering

A convenient measure for deviation from the pure rotational behavior is the signature-splitting index $S(L)$ [27]:

$$S(L) = \frac{[E_{L+1} - E_L] - [E_L - E_{L-1}]}{E_{2_1^+}}, \quad (16)$$

which vanishes for

$$E(L) = E_0 + AL(L+1), \quad (17)$$

but not for

$$E(L) = E_0 + AL(L+1) + B[L(L+1)]^2. \quad (18)$$

Another quantity is also used in practice [28]

$$\Delta E_{\gamma,1}(L) = \frac{1}{16}(6\Delta E(L) - 4\Delta E(L-1) - 4\Delta E(L+1) + \Delta E(L+2) + \Delta E(L-2)), \quad (19)$$

where $\Delta E(L) = E(L) - E(L-1)$. The staggering function (19), in contrast to (16), vanishes for (18) and hence it represents a more sensitive measure for the deviations

of the nuclear dynamics from that of collective rotational motion. We recall that the SU(3) limit of the spdf-IBM predicts [28] a constant behavior for the staggering function (19), thus being unable to describe the latter.

In the present work we consider the odd-even staggering between the states of the GSB and $K^\pi = 0^-$ band. The mapping of the experimentally observed states of the two bands under considerations onto the basis states of Table I ("stretched approximation") establishes the relation between the quantum numbers N and L . As a result, the energies of the GSB can be expressed in the form [14]:

$$E(L) = \beta L(L+1) + \gamma L, \quad (20)$$

whereas those of the $K^\pi = 0^-$ band as

$$E(L) = \beta L(L+1) + (\gamma + \eta)L + \xi. \quad (21)$$

The relation between the new set of parameters entering in Eqs.(20) and (21) and that in Eq.(15) is given in Ref.[14]. From the expressions (20)-(21), one can see that the energies of the GSB and $K^\pi = 0^-$ band consist of rotational $L(L+1)$ and vibrational L terms. The rotational interaction is with equal strength β in both of the bands.

The calculated and experimental staggering patterns for all considered nuclei are illustrated in Fig.2. As can be seen the IVBM describes well the energy staggering, including the "beat patterns" (^{226}Ra). The first "beat pattern" appears at the point where the two bands are crossing. In order to be able to describe the second "beat pattern" we assume that the states with high angular momentum ($L \geq 20$) of the yrast band are members of the first excited β -band. The correct reproduction of the experimental energy staggering, including the "beat patterns", is due to the mixing of different collective modes (see Eqs.(20) and (21)) within the framework of the symplectic IVBM. The mixing of the two bands under consideration is caused by the L -dependent interaction term ηL in (21).

C. Transition probabilities

It is well known that the transition probabilities are a more sensitive test for each model. Negative parity states of the $K^\pi = 0^-$ band are characterized by the enhanced $E1$ transition strengths to the GSB. In the present work we consider only the $B(E1)$ and $B(E2)$ transition probabilities concerning the ground state and $K^\pi = 0^-$ bands.

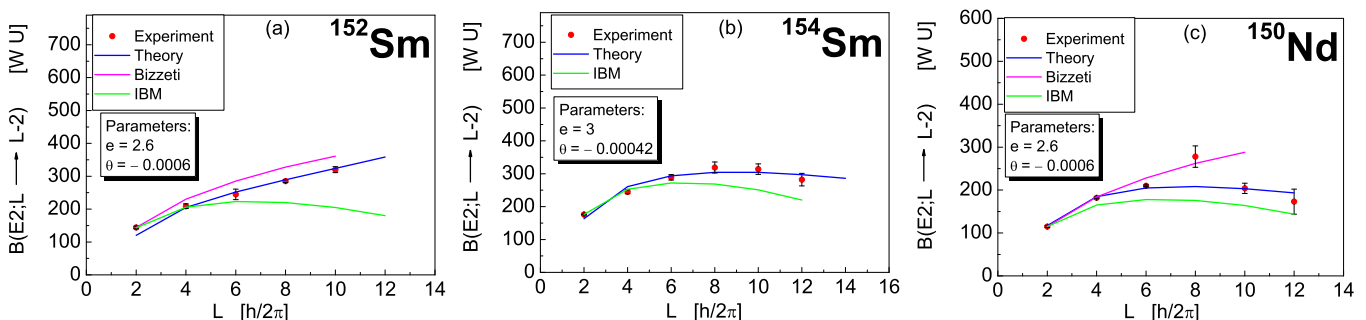


FIG. 3: (Color online) Comparison of theoretical and experimental values for the transition probabilities of the intraband $E2$ transitions in the ground state band in ^{152}Sm , ^{154}Sm , and ^{150}Nd . For comparison, the theoretical predictions of some other collective models are also shown.

The transition probabilities between the collective states attributed to the basis states of the Hamiltonian are by definition the square of the SO(3) reduced matrix elements of the transition operators:

$$B(E\lambda; L_i \rightarrow L_f) = \frac{1}{2L_i + 1} |\langle f || T^{E\lambda} || i \rangle|^2. \quad (22)$$

The general approach for calculating the transition probabilities along the considered dynamical symmetry is given in Ref.[29], where the $B(E2)$ transition probabilities between the states of the GSB were calculated. Similarly, in the present work we calculate the strengths of the

intraband $E2$ transitions in both the GSB and $K^\pi = 0^-$ band, as well as the interband $E1$ transitions connecting the states of these two bands. In our calculations, we use the following operators

$$T^{E2} = e \left[A_{(1,1)[0]_2}^{[1,-1]_6} \begin{matrix} 20 \\ 00 \end{matrix} + \theta \left([F \times F]_{(0,2)[0]_2}^{[4]_6} \begin{matrix} 20 \\ 00 \end{matrix} + [G \times G]_{(2,0)[0]_2}^{[-4]_6} \begin{matrix} 20 \\ 00 \end{matrix} \right) \right], \quad (23)$$

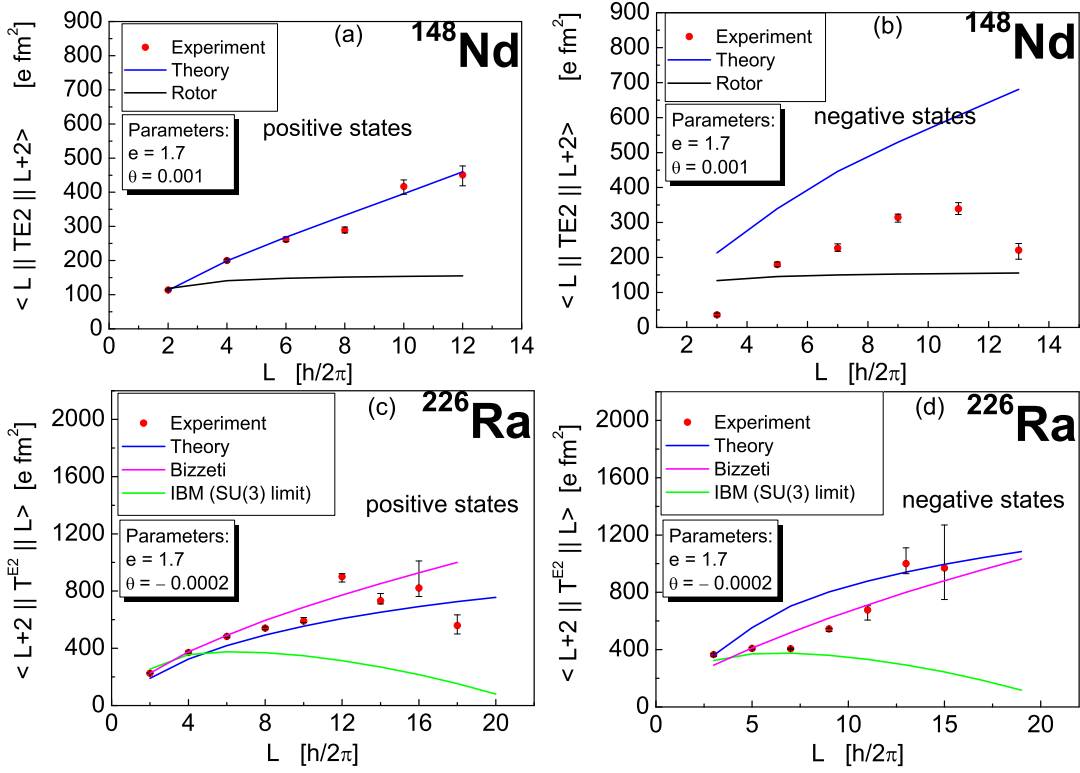


FIG. 4: (Color online) Comparison of theoretical and experimental values for the matrix elements of the intraband $E2$ transitions in the ground state band and $K^\pi = 0^-$ band in ^{148}Nd and ^{226}Ra . For comparison, the theoretical predictions of some other collective models are also shown.

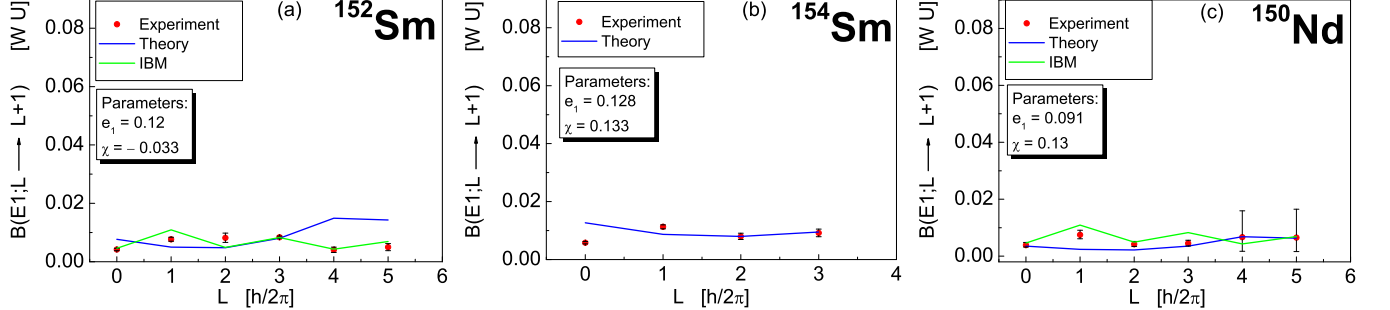


FIG. 5: (Color online) Comparison of theoretical and experimental values for the transition probabilities of the interband $E1$ transitions between the states of the GSB and $K^\pi = 0^-$ band in ^{152}Sm , ^{154}Sm , and ^{150}Nd . For comparison, the theoretical predictions of some other collective models are also shown.

and

$$T^{E1} = e_1 \left[A_{(1,1)[2]_2}^{[1,-1]_6} \begin{matrix} 10 \\ 1-1 \end{matrix} + \chi \left([F \times F]_{(2,1)[2]_2}^{[4]_6} \begin{matrix} 10 \\ 11 \end{matrix} + [G \times G]_{(1,2)[-2]_2}^{[-4]_6} \begin{matrix} 10 \\ 1-1 \end{matrix} \right) \right], \quad (24)$$

as transition operators for the $E2$ and $E1$ transitions, respectively. In (23) and (24) explicit tensor properties with respect to the reduction chain (4) are written. For more details concerning the calculations we refer the reader to Ref.[29].

In Fig.3 we compare our theoretical results for the transition probabilities of the intraband $E2$ transitions in the

ground state band for the three isotopes ^{152}Sm , ^{154}Sm , and ^{150}Nd . In Fig.4 the comparison of the theoretical matrix elements of the intraband $E2$ transitions in both ground state band and $K^\pi = 0^-$ band for ^{148}Nd and ^{226}Ra nuclei with experiment is given. For comparison, the theoretical predictions of some other collective models are also shown. We see that IVBM describes reasonably well the general trend of the experimental data. An enhancement of the theoretical $E2$ matrix elements in the $K^\pi = 0^-$ band compared to the GSB values is obtained. Such an enhancement was experimentally observed in ^{144}Ba [30].

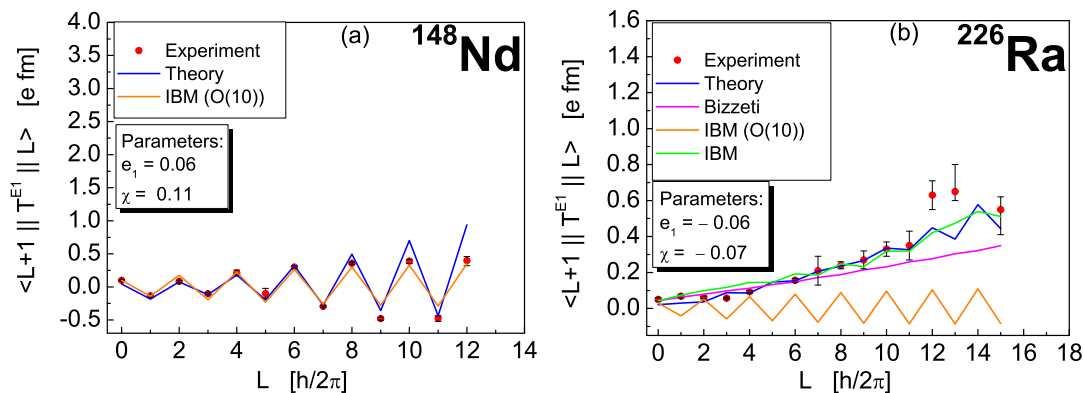


FIG. 6: (Color online) Comparison of theoretical and experimental values for the matrix elements of the interband $E1$ transitions between the states of the GSB and $K^\pi = 0^-$ band in ^{148}Nd and ^{226}Ra . For comparison, the theoretical predictions of some other collective models are also shown.

In Figs.5 and 6 the calculated transition strengths (matrix elements or transition probabilities) for the $E1$ transitions connecting the states of the GSB and $K^\pi = 0^-$ band are compared with experiment [1], [31] (^{226}Ra), [32] (^{148}Nd) and the predictions of some other collective models incorporating octupole or/and dipole degrees of freedom.

An interesting zigzagging behavior of the matrix elements of the $E1$ transitions is observed in the case of ^{148}Nd . Such a staggering behavior with correct phases is obtained in the framework of the spdf-IBM if as a transition operator is used the O(10) generator. Equivalent picture is obtained if the O(4) generator is used as a transitional operator instead of the O(10) one. From the Fig.6 one sees that IVBM is also able to describe such staggering behavior.

IV. CONCLUSIONS

In the present work the low-lying spectra including the first few excited positive and negative parity bands of some heavy even-even nuclei from the rare earth and actinide mass regions, namely ^{152}Sm , ^{154}Sm , ^{148}Nd , ^{150}Nd , ^{226}Ra and ^{230}Th , are investigated within the framework

of the symplectic Interacting Vector Boson Model with $\text{Sp}(12, R)$ dynamical symmetry group. Symplectic dynamical symmetries allow the change of the number of excitation quanta or phonons building the collective states providing for larger representation spaces and richer sub-algebraic structures to incorporate more complex nuclear spectra. The theoretical predictions for the energy levels, energy staggering and transition strengths between the collective states are compared with experiment and some other collective models incorporating octupole degrees of freedom. The IVBM describes well the experimental data including some structural effects observed in the nuclear spectra, like the "beat patterns" (^{226}Ra) in the energy staggering. The results obtained for the energy levels, the energy staggering and the transition strengths in the considered nuclei prove the correct mapping of the basis states to the experimentally observed ones and reveal the relevance of the used dynamical symmetry of IVBM in the simultaneous description of the low-lying positive and negative parity bands.

References

-
- [1] National Nuclear Data Center (NNDC), <http://www.nndc.bnl.gov/>
- [2] P. A. Butler and W. Nazarewicz, *Rev. Mod. Phys.* **68**, 349 (1996).
- [3] A. Bohr and B. R. Mottelson, *Nucl. Phys.* **4**, 529 (1957).
- [4] F. Iachello and A. Arima, *The Interacting Boson Model* (Cambridge University Press, Cambridge, 1987).
- [5] C. S. Han *et al.*, *Phys. Lett.* **B163**, 295 (1985).
- [6] J. Engel and F. Iachello, *Phys. Rev. Lett.* **54**, 1126 (1985); J. Engel and F. Iachello, *Nucl. Phys.* **A472**, 61 (1987).
- [7] F. Iachello and A. D. Jackson, *Phys. Lett.* **B108**, 151 (1982); F. Iachello, *Nucl. Phys.* **A396**, 233c (1983); H. Daley and F. Iachello, *Phys. Lett.* **B131**, 281 (1983); H. J. Daley and F. Iachello, *Ann. Phys.* **167**, 73 (1986).
- [8] T. M. Shneidman *et al.*, *Phys. Lett.* **B526**, 322 (2002).
- [9] P. G. Bizzeti and A. M. Bizzeti-Sona, *Phys. Rev.* **C70**, 064319 (2004).
- [10] P. G. Bizzeti and A. M. Bizzeti-Sona, *Phys. Rev.* **C77**, 024320 (2008).
- [11] P. G. Bizzeti and A. M. Bizzeti-Sona, *Phys. Rev.* **C81**, 034320 (2010).
- [12] D. Bonatsos *et al.*, *Phys. Rev.* **C71**, 064309 (2005); D. Lenis and D. Bonatsos, *Phys. Lett.* **B633**, 474 (2006).

- [13] A. Georgieva, P. Raychev, and R. Roussev, J. Phys. **G8**, 1377 (1982).
- [14] H. Ganey, V. P. Garistov, and A. I. Georgieva, Phys. Rev. **C69**, 014305 (2004).
- [15] V. Bargmann and M. Moshynsky, Nucl. Phys. **18**, 697 (1960).
- [16] V. Bargmann and M. Moshynsky, Nucl. Phys. **23**, 177 (1961).
- [17] M. Moshinsky and C. Quesne, J. Math. Phys. **11**, 1631 (1970).
- [18] J. P. Elliott, Proc. Roy. Soc. **A254**, 128, 526 (1958).
- [19] D. J. Rowe, Rep. Prog. Phys. **48**, 1419 (1985).
- [20] H. J. Lipkin, Nucl. Phys. **A 350**, 16 (1980).
- [21] M. Babilon *et al.*, Phys. Rev. **C72**, 064302 (2005).
- [22] M. Elvers *et al.*, Phys. Rev. **C84**, 054323(2011).
- [23] N. V. Zamfir and D. Kusnezov, Phys. Rev. **C 63**, 054306 (2001).
- [24] H. Y. Ji *et al.*, Nucl. Phys. **A 658**, 197 (1999); G. L. Long *et al.*, Phys. Rev. **C57**, 2301 (1998).
- [25] R. F. Casten and N. V. Zamfir, Phys. Rev. Lett. **87**, 052503 (2001).
- [26] K. Nomura, D. Vretenar, and B. N. Lu, Phys. Rev. **C88**, 021303(R) (2013).
- [27] N. V. Zamfir, P. von Brentano, and R. F. Casten, Phys. Rev. **C49**, R605 (1994).
- [28] D. Bonatsos *et al.*, Phys. Rev. **C62**, 024301 (2000).
- [29] H. G. Ganey and A. I. Georgieva, Phys. Rev. **C76**, 054322 (2007).
- [30] T. M. Shneidman *et al.*, Eur. Phys. J. **A25**, 387 (2005).
- [31] H. J. Wollersheim *et al.*, Nucl. Phys. **A556**, 261(1993).
- [32] R. W. Ibbotson *et al.*, Nucl. Phys. **A619**, 213 (1997).